Bulk and surface nucleation of the order-disorder transition in Cu_3Au

1998 J. Phys.: Condens. Matter 10 45

(http://iopscience.iop.org/0953-8984/10/1/006)

J. Phys.: Condens. Matter **10** (1998) 45–60. Printed in the UK PII: S0953-8984(98)86471-0

Bulk and surface nucleation of the order–disorder transition in Cu_3Au

Chaok Seok and David W Oxtoby

Department of Chemistry and James Franck Institute, The University of Chicago, 5640 South Ellis Avenue, Chicago, IL 60637, USA

Received 31 July 1997

Abstract. Bulk and surface nucleation of the order–disorder transition in Cu_3Au have been studied using a lattice version of density functional theory. The surface transitions at three different surfaces, (001), (011), and (111), are discussed. The surface-induced disorder transition does not occur at the (001) surface even when the surface transition is continuous and the bulk is discontinuous if only nearest-neighbour interactions are included. The results for the nucleation rates are compared with experiment.

1. Introduction

Cu_3Au is a classical example of a binary alloy that undergoes an order–disorder transition ($T_{tr} = 663$ K) to form a substitutionally disordered phase well below its melting temperature ($T_m = 1226$ K). Below the transition temperature, the crystal exists in its ordered state where gold atoms occupy the corner positions, and copper the face positions in a face-centred cubic lattice. Above T_{tr}, the fcc lattice is maintained, but the gold and copper atoms randomly occupy the lattice sites.

Many experimental and theoretical studies have focused on the role of the surface in Cu_3Au since it was found that the (001) surface undergoes a second-order transition at the temperature that is also the bulk transition temperature [1–5], whereas the bulk transition is first order [6, 7]. Because surface atoms have a smaller number of neighbours than bulk ones, the surface may begin to disorder below the bulk transition temperature if the interactions between the surface atoms are weak compared to those for bulk ones. If the surface disorders when the bulk is still ordered, the disorder at the surface may propagate several layers below the surface, and the thickness of the disordered layers may increase as the transition temperature is approached. Within Landau theory [8], this phenomenon can occur when the surface transition is continuous and the bulk is discontinuous. The thickness of the disordered layers increases logarithmically as T_{tr} is approached and diverges as T_{tr} is approached, so the bulk disorder is induced by the surface. This surface-induced disordering is in close analogy to the surface melting at a crystal–vapour interface where structural (not compositional) disordering occurs.

Surface transitions in Cu_3Au have been studied using surface-sensitive techniques such as low-energy electron diffraction (LEED) [1, 2], spin-polarized LEED [3, 4], helium-atom scattering [5], low-energy-ion scattering (LEIS) [9], and x-ray scattering at grazing angles [10–12]. Surface order parameters as well as surface compositions have been measured as functions of the temperature. In experiments studying the dynamics of the transition, a

0953-8984/98/010045+16$19.50

sample is quenched from a high temperature above T_{tr} to below T_{tr}, and the time evolution of the superlattice peak is monitored. The short-time dynamics is dominated by nucleation and growth, and the long-time dynamics by coarsening of antiphase domains. The long-time behaviour in bulk has been well studied both experimentally and theoretically because of the interesting universal scaling behaviour in both time and space [13–15]. However, there has not been much theoretical study of the earlier-time dynamics in Cu_3Au. The surface dynamics has also been studied, and it was found that the (001) surface orders much more quickly than the bulk [2, 5] while the (011) [16] and (111) [11] surfaces order slowly.

In this paper, we study bulk and surface nucleation using a density functional theory in statistical mechanics. Nucleation is the initial stage of ordering or disordering when the sample is undercooled or superheated to a metastable state, and can be very slow for a small degree of undercooling or superheating. We employ the same formalism used in our previous study of equilibrium properties of Cu_3Au [17]. It is based on the lattice analogue of density functional theory, developed by Dieterich and co-workers [18], and extended by us to a two-component system. Nearest-neighbour pair and three-body interactions are employed. Our theory gives a good bulk transition temperature when a set of empirical potential parameters is used, as in [17]. We examine both equilibrium properties and nucleation at the (001), (011), and (111) surfaces and compare them. Because of the different structure near the different surfaces, the surface transition and nucleation at the (001) surface are distinctively different from the others in our theory. The (011) and (111) surface can undergo surface-induced disordering for some parameters. However, the (001) surface is decoupled from the bulk, and shows no surface-induced disordering even when the surface transition is second order. Nucleation barriers are found by locating saddle points on the grand canonical potential surface. Formation of ordered nuclei at a free surface in a surface-induced disorder transition is highly disfavoured because the surface favours disordering. The critical nuclei can form just under the surface, but not in contact with the surface. In contrast to this, the nucleation barrier at the (001) surface can be much lower than in the bulk. These results are compared with experiment.

The outline of this paper is as follows. In section 2, theories used in this study are described. Specifically, the lattice analogue of density functional theory is reviewed in subsection 2.1, additional surface parameters are discussed in 2.2, and classical and density functional nucleation theories are presented in 2.3. Section 3 presents results and a discussion for bulk (subsection 3.1) and surface (subsections 3.2 and 3.3) transitions and for nucleation. Section 4 gives conclusions.

2. Theory

2.1. The lattice analogue of density functional theory

We employ the grand canonical ensemble where T, V, and μ are constant. The grand canonical potential Ω for a lattice system is

$$\Omega(\{n_i^c, n_i^g\}) = F_{id}(\{n_i^c, n_i^g\}) + F_{exc}(\{n_i^c, n_i^g\}) - \sum_i (\mu^c n_i^c + \mu^g n_i^g) \tag{1}$$

where subscripts denote lattice sites, i, j,..., and superscripts denote the kind of atom that occupies each lattice site, c for copper and g for gold for a Cu_3Au system. For example, n_i^c is the probability that a copper atom occupies site i, and μ^c is the chemical potential of copper. The free energy is divided into an ideal term and an excess term. The excess free energy is approximated as an expansion around a reference state and truncated at third

order:

$$F_{exc} = F_{exc,ref} - \beta^{-1} \sum_{\nu=c,g} \sum_{i} c_1^{\nu} \Delta n_i^{\nu} - \frac{\beta^{-1}}{2!} \sum_{\nu,\mu=c,g} \sum_{i,j} c_2^{\nu\mu}(i,j)\, \Delta n_i^{\nu}\, \Delta n_j^{\mu} - \frac{\beta^{-1}}{3!} \sum_{\nu,\mu,\lambda=c,g} \sum_{i,j,k} c_3^{\nu\mu\lambda}(i,j,k)\, \Delta n_i^{\nu}\, \Delta n_j^{\mu}\, \Delta n_k^{\lambda} \tag{2}$$

where $\Delta n_i^{\nu} = n_i^{\nu} - n_{i,ref}^{\nu}$. The expansion coefficients, which are the direct correlation functions, are determined using a mean-spherical approximation (MSA) and the Ornstein–Zernike equation, as in reference [17].

The above formalism reduces to that of an effective one-component system if vacancies can be ignored. For bulk,

$$\beta\Omega = \sum_i [n_i^c \ln n_i^c + (1-n_i^c)\ln(1-n_i^c)] - \sum_i \ln[n^c/(1-n^c)]\, \Delta n_i^c - \frac{1}{2!} \sum_{i,j} A^{(2)}(i,j)\, \Delta n_i^c\, \Delta n_j^c - \frac{1}{3!} \sum_{i,j,k} A^{(3)}(i,j,k)\, \Delta n_i^c\, \Delta n_j^c\, \Delta n_k^c \tag{3}$$

where

$$\begin{aligned} A^{(2)}(i,j) &= c_2^{cc}(i,j) + c_2^{gg}(i,j) - 2c_2^{cg}(i,j) \\ A^{(3)}(i,j,k) &= c_3^{ccc}(i,j,k) - 3c_3^{ccg}(i,j,k) + 3c_3^{cgg}(i,j,k) - c_3^{ggg}(i,j,k). \end{aligned} \tag{4}$$

With the MSA and a nearest-neighbour approximation,

$$\begin{aligned} A^{(2)}(i,j) &= -\beta V^{(2)} \qquad \text{if } i, j \text{ are NN} \\ A^{(3)}(i,j,k) &= -\beta V^{(3)} \qquad \text{if } i, j, k \text{ are NN} \end{aligned} \tag{5}$$

where

$$\begin{aligned} V^{(2)} &= \upsilon^{cc} + \upsilon^{gg} - 2\upsilon^{cg} \\ V^{(3)} &= \upsilon^{ccc} - 3\upsilon^{ccg} + 3\upsilon^{cgg} - \upsilon^{ggg} \end{aligned} \tag{6}$$

and $\upsilon^{\nu\mu}$ are the nearest-neighbour pair potentials for species ν and μ, and $\upsilon^{\nu\mu\lambda}$ are the three-body potentials when all three atoms are nearest neighbours. $A^{(2)}(i,i)$ is calculated from the Ornstein–Zernike equation, and $A^{(3)}(i,i,i)$ and $A^{(3)}(i,i,j)$ are set to zero.

Equilibrium states are found by minimizing Ω using the following iteration scheme:

$$(n_\lambda^{\nu})_{i+1} = (n_\lambda^{\nu})_i - d \left.\frac{\partial\Omega}{\partial n_\lambda^{\nu}}\right|_{\{n_\lambda^{\nu}\}_i} \tag{7}$$

where the step size d is chosen to speed convergence.

2.2. Surface transitions

We consider the (001), (011), and (111) surfaces here, whose structures are shown in figure 1. In the [001] and [011] directions, there are two kinds of alternating plane: planes with 50% Cu sites and 50% Au sites (Cu–Au layers) and planes with only Cu sites (Cu layers). It is known that the outermost (001) and (011) surfaces are Cu–Au layers. In the [111] direction, all planes have 75% Cu and 25% Au sites. The nearest neighbours for surface atoms are shown in the figures. We define the order parameter as the difference between the probability that an atom occupies a correct site and the probability that it occupies a wrong site (in terms of the perfectly ordered state). Therefore, the order parameter for each layer is $n_{c,l}^c - n_{g,l}^c$, where l is the layer number, and those for Cu layers are not defined.

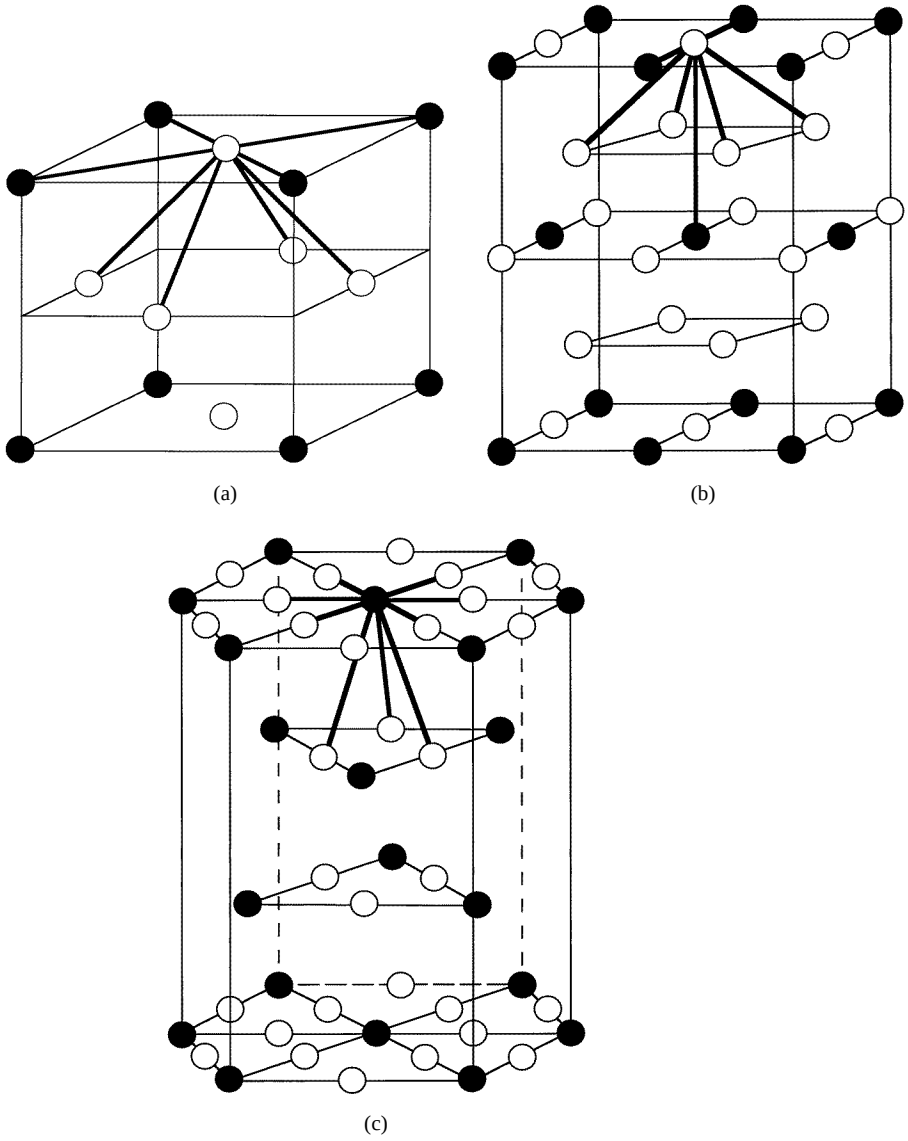

Figure 1. Structures of the different surfaces (a) (001), (b) (011), and (c) (111). Black circles denote Au sites and white circles Cu sites. The top layers are the free surfaces. Nearest neighbours are connected by thicker lines, and the distance between them is $\sqrt{2}/2a$. The sides perpendicular to the surfaces are elongated in (b) and (c) for a clearer view. The distances between the adjacent layers are (a) $1/2a$, (b) $\sqrt{2}/4a$, and (c) $\sqrt{3}/3a$.

For bulk calculations, a disordered bulk is used as a reference, or $n^c_{i,ref} = 0.75$. If the same reference state is used for the surface, effective surface field (F) and surface enhancement (I) terms arise because of the missing bonds:

$$\beta\Omega = \sum_i [n_i^c \ln n_i^c + (1 - n_i^c)\ln(1 - n_i^c)] - \sum_i{}' \ln[n^c/(1 - n^c)]\,\Delta n_i^c + \beta F \sum_i{}^s \Delta n_i^c$$

$$- \frac{1}{2!}\sum_{i,j}{}' A^{(2)}(i,j)\,\Delta n_i^c\,\Delta n_j^c + \frac{\beta I}{2!}\sum_{i,j}^{s}\Delta n_i^c\,\Delta n_j^c$$
$$- \frac{1}{3!}\sum_{i,j,k}{}' A^{(3)}(i,j,k)\,\Delta n_i^c\,\Delta n_j^c\,\Delta n_k^c \tag{8}$$

where $\sum'$ stands for a summation over occupied lattice sites and $\sum^s$ for a summation over surface sites. F and I are expressed in terms of only bulk potential parameters as follows:

$$F = -u[n^c(\upsilon^{cc} - \upsilon^{cg}) + n^g(\upsilon^{cg} - \upsilon^{gg})] + v[n^c n^c(\upsilon^{ccc} - \upsilon^{ccg}) + 2n^c n^g(\upsilon^{ccg} - \upsilon^{cgg}) + n^g n^g(\upsilon^{cgg} - \upsilon^{ggg})] \tag{9}$$

$$I = -w[n^c(\upsilon^{ccc} - 2\upsilon^{ccg} + \upsilon^{cgg}) + n^g(\upsilon^{ccg} - 2\upsilon^{cgg} + \upsilon^{ggg})] \tag{10}$$

where the occupation numbers for the reference state are $n^c = 0.75$ and $n^g = 0.25$, and $(u, v, w) = (4, 4, 2)$, $(5, 6, 3)$, and $(3, 3, 2)$ for the (001), (011), and (111) surfaces, respectively. F determines which species segregates at the surface, and I affects the order parameter at the surface, as will be discussed later.

The use of a bulk reference state for a surface problem may not be a good approximation. A surface reference state was therefore introduced in reference [17]; it is disordered and has constant layer composition. In this case, $A^{(2)}_{surf}(1)$ corresponds to $A^{(2)}(1) - \beta I$ above, and F and $A^{(2)}(i,i)$ depend on layer number. The field for the lth layer is

$$\begin{aligned}-\beta F_l' = &-n^c\{c_\infty^{cc}(0) - c_\infty^{cg}(0)\} - n^g\{c_\infty^{cg}(0) - c_\infty^{gg}(0)\} \\ &+ n^c\{c_l^{cc}(0) - c_l^{cg}(0)\} + n^g\{c_l^{cg}(0) - c_l^{gg}(0)\} \\ &- \delta_{l,0}u[2n^c\{c_2^{cc}(1) - c_2^{cg}(1)\} + 2n^g\{c_2^{cg}(1) - c_2^{gg}(1)\} \\ &- n^c\{c_{2,surf}^{cc}(1) - c_{2,surf}^{cg}(1)\} - n^g\{c_{2,surf}^{cg}(1) - c_{2,surf}^{gg}(1)\}] - \delta_{l,0}\beta F_{3\text{-}body}\end{aligned} \tag{11}$$

where

$$\begin{aligned}-\beta F_{3\text{-}body} = 3v[&n^c n^c\{c_3^{ccc}(1) - c_3^{ccg}(1)\} + 2n^c n^g\{c_3^{ccg}(1) - c_3^{cgg}(1)\} \\ &+ n^g n^g\{c_3^{cgg}(1) - c_3^{ggg}(1)\}]].\end{aligned} \tag{12}$$

$c_l(0) = c_2(i,i)$ with i on the lth layer, and the argument '1' is used when the relevant lattice sites are nearest neighbours. Although there appear to be more parameters to be fitted to the experimental data if a surface reference state is used, the change of many parameters affects the results only through the surface enhancement and the surface field, because the $c_l(0)$ are not very different from the bulk value except at the surface. Therefore, only a bulk reference state will be used for surface calculations here.

2.3. Nucleation

In classical nucleation theory, the nucleation barrier is given by

$$\Delta\Omega^* = \frac{16}{3}\pi\frac{\gamma^3}{\Delta G^2} \tag{13}$$

where γ is the planar surface tension and ΔG is the free-energy difference of the two phases. It is obtained by maximizing $\Delta\Omega$ for a spherical droplet, which is bulk-like inside the droplet, and has an interface with planar surface tension. When the nucleation occurs at a surface, the critical nucleus is a spherical cap with contact angle θ determined by the planar interfacial tensions at coexistence,

$$\cos\theta = \frac{\gamma_{\alpha v} - \gamma_{\beta v}}{\gamma_{\alpha\beta}} \tag{14}$$

where $\gamma_{\alpha v}$ is the surface tension for the α–v interface, etc, and α and β denote the two phases (ordered and disordered) and v the vacuum. The contact angle is close to 0° if surface nucleation is more favoured than bulk nucleation, and to 180° if nucleation at the surface is disfavoured. In the case of surface-induced disordering, because the disordered phase intervenes between the surface and the ordered bulk ('wets' the surface), the surface tension of the ordered system $\gamma_{\alpha v}$ is the sum of the surface tension of the disordered system $\gamma_{\beta v}$ and the interfacial tension between the ordered and disordered phases $\gamma_{\alpha\beta}$. The contact angle is then 0° from equation (14).

In a density functional approach, the critical nucleus is identified as a saddle point on the grand canonical potential surface. We determine this point by iteration, starting with an appropriate initial profile. The procedure for finding the saddle point using an iteration method is described in [19]. Smaller initial nuclei shrink, and larger ones grow indefinitely upon iteration. The intermediate profile reaches a quasistationary state, which is identified as the critical nucleus.

The nucleation rate per unit time and volume is determined from the classical expression,

$$J = J_0 \mathrm{e}^{-\Delta\Omega^*/kT} \tag{15}$$

where the prefactor J_0 depends on the mechanism of particle attachment to clusters of the new phase. In the order–disorder transition, diffusion by a vacancy mechanism would be responsible for atomic transport, and the prefactor is given by

$$J_0 = 4Zn_s^* a^{-5} D_0 \mathrm{e}^{-\Delta H_d/kT} \tag{16}$$

where Z is the Zeldovich factor [20], n_s^* is the number of atoms at the surface of the critical nucleus, a is the conventional lattice parameter, D_0 is the prefactor for the diffusion coefficient, and ΔH_d is the enthalpy barrier for diffusion. $a = 4$ Å [5], $D_0 = 0.1$ cm^2 s^{-1}, and $\Delta H_d = 46$ kcal mol^{-1} [21] are used.

3. Results and discussion

3.1. Bulk nucleation

When a system is undercooled or superheated by a small amount, the original phase becomes metastable, but a barrier must be overcome in order to form the new phase. The disordered (ordered) phase becomes no longer metastable but unstable beyond the lower (upper) spinodal temperature, and the nucleation barrier vanishes. The lower spinodal temperature is determined experimentally by measuring the short-range order intensity at the superlattice peak at high temperatures and extrapolating to the spinodal temperature where it diverges. The relative spinodal temperature determined is $(T_{tr} - T_{sp})/T_{tr} = 0.051$ in [22] and 0.036 in [23]. Our calculation gives no lower spinodal, although the system approaches the spinodal asymptotically. However, we obtained surface spinodals close to T_{tr}, as will be shown in subsection 3.2. Because any real sample has surfaces, it is not possible to measure the true bulk spinodal if the surface spinodal is closer to T_{tr}. Therefore, our results are not inconsistent with experiments. We find an upper spinodal at $(T_{sp} - T_{tr})/T_{tr} = 0.056$ when $V^{(3)}/V^{(2)} = 0.1$, but there are no experimental data on the upper spinodal.

We calculate the nucleation barrier and rate as discussed in subsection 2.3. Equation (3) is used for the grand canonical potential. Since we can express the temperature in units of $V^{(2)}/k_B$, and other potential parameters in units of $V^{(2)}$, only $V^{(3)}/V^{(2)}$ needs to be determined, where $V^{(2)}$ and $V^{(3)}$ are defined in equation (6). $V^{(3)}/V^{(2)} = 0.1$ is used for all of the following bulk and surface calculations. A critical nucleus can be centred

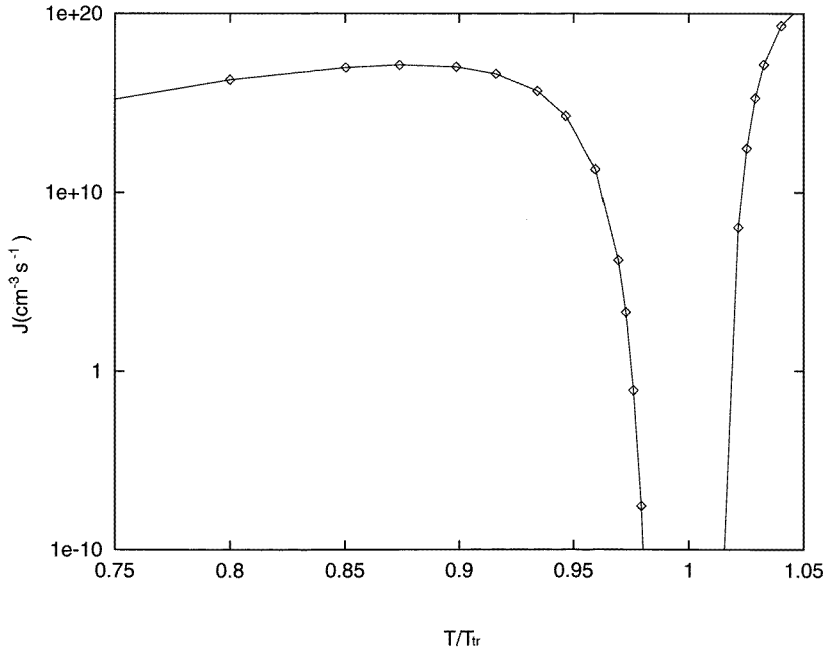

Figure 2. The bulk nucleation rate J as a function of temperature.

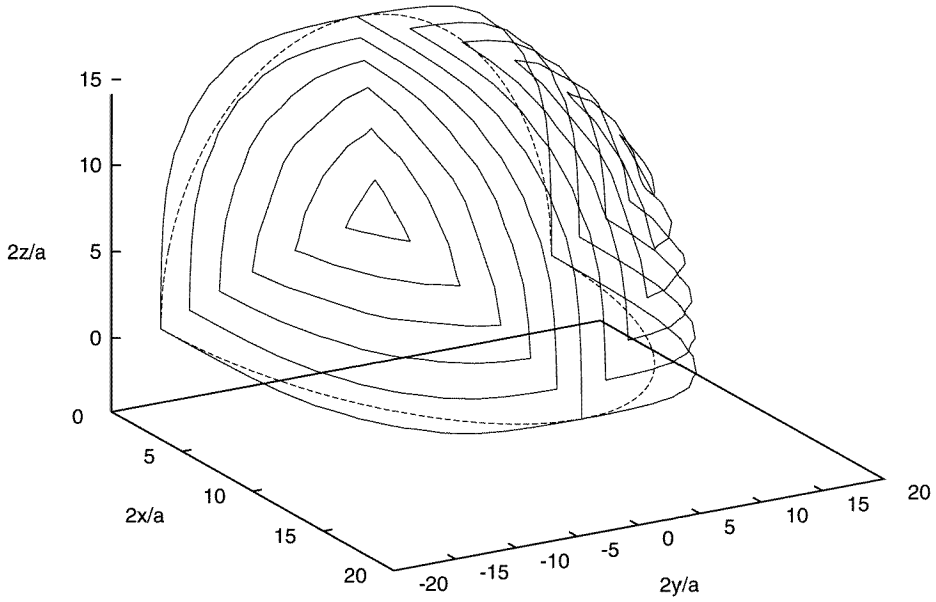

Figure 3. Contours of constant occupation number for a critical nucleus at $T = 0.947T_{tr}$. x, y, and z are distances from the centre of the nucleus. The dashed curve for a sphere is a guide to the eye. It can be seen that the surface perpendicular to the [001] and equivalent directions is flatter than that of a sphere.

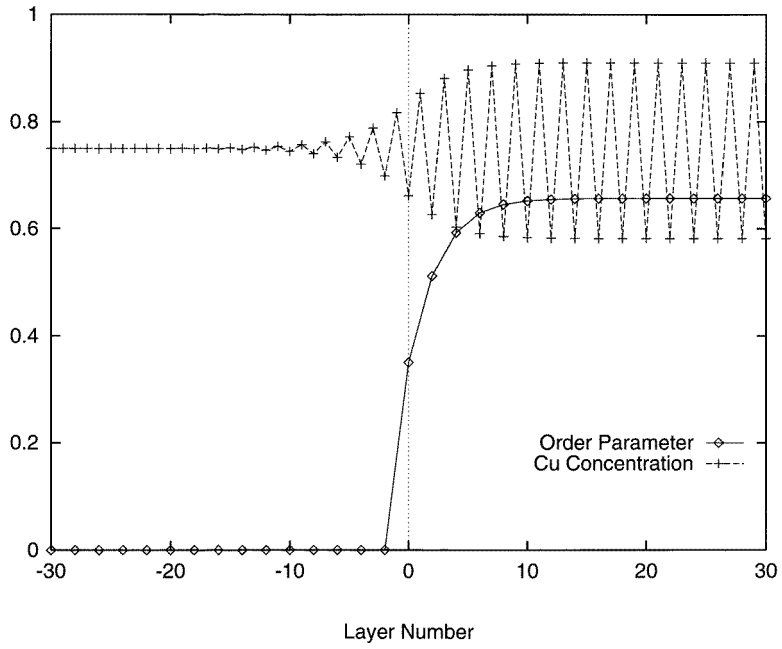

(a)

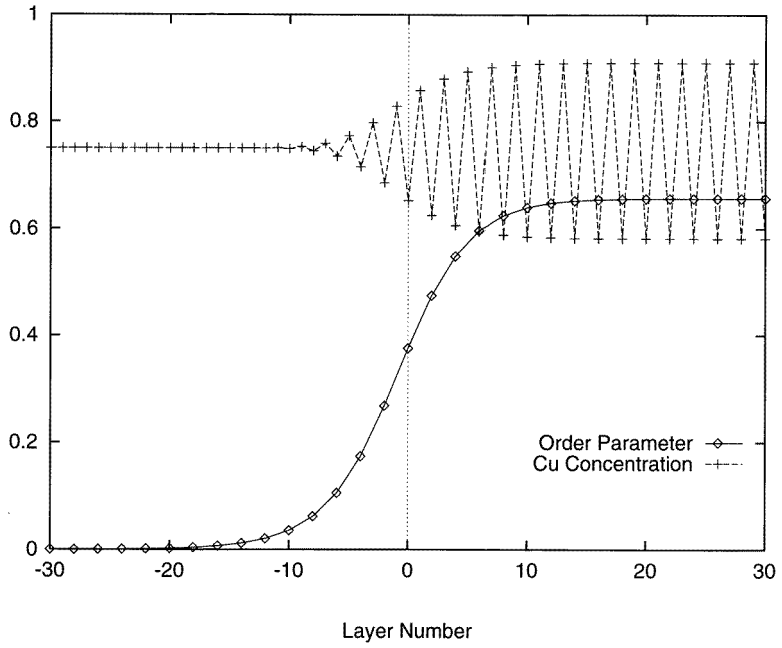

(b)

Figure 4. Order parameter and Cu concentration profiles between the ordered and the disordered phases at coexistence in the (a) [001], (b) [011], and (c) [111] directions.

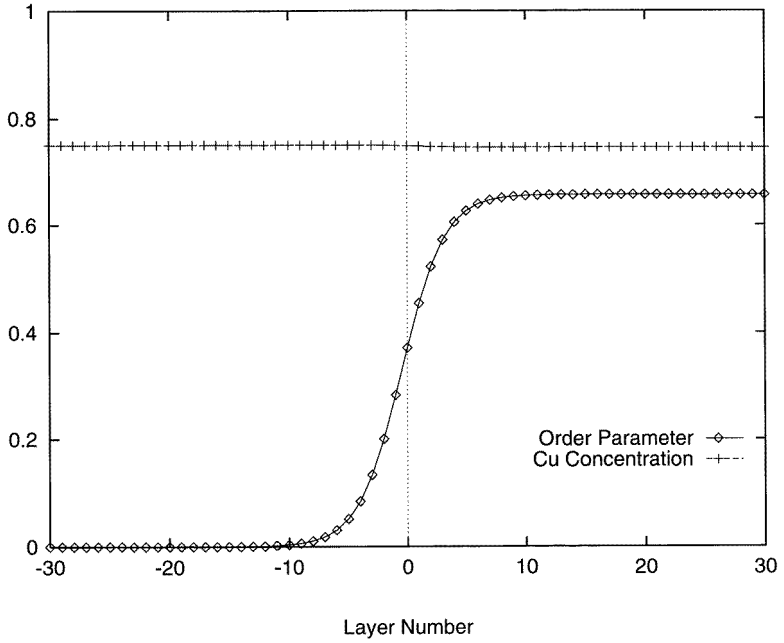

(c)

Figure 4. (Continued)

on any one of four sublattices (three Cu sublattices and one Au sublattice) or off-lattice points. We found that nuclei centred on Au sites have lower barriers than those on Cu sites, especially for smaller nuclei. This is understandable when one notes that Au has more unlike nearest neighbours (twelve Cu) than Cu (four Au and eight Cu) in the ordered phase, and that the interaction between unlike neighbours is stronger in a system that undergoes an order–disorder transition.

The bulk nucleation rate calculated from equations (15) and (16) has a maximum at some temperature below T_{tr}, as shown in figure 2. This occurs because of the opposing effects of the nucleation barrier and diffusion. The nucleation barrier decreases as the temperature is lowered, but the diffusion becomes slower at low temperatures. The nucleation rate is very fast, except for very small degrees of undercooling or superheating, which is in agreement with experiments. Nucleation becomes slower only at undercoolings of $\Delta T/T \approx 0.008$, according to experiment [13, 24]. Our results show that nucleation becomes of the order of 1 cm^{-3} s^{-1} at $\Delta T/T \approx 0.025$ for undercooling, and $\Delta T/T \approx 0.019$ for superheating for $V^{(3)}/V^{(2)} = 0.1$. As will be discussed in the next subsection, we found that nucleation at the (001) surface is faster than that in the bulk. When surface nucleation is fast enough, the surface nuclei can grow into the bulk before critical nuclei form in the bulk, and the experimentally measured range of slow nucleation will be narrower than that predicted from the bulk nucleation rate. Nucleation is so fast because of the low free energy of the interface between ordered and disordered phases (see equation (13)); it is about 10% of the liquid–solid interfacial tension of the Lennard-Jones fluid, which in turn is about 10% of that of a typical gas–liquid interface.

Classical theory is supposed to be correct in the limit of large critical nuclei, where the inside is close to bulk and the interface close to planar. This is not the case here, however;

the critical nuclei are not spherical because the free energy of the interface between ordered and disordered phases depends on direction, unlike gas–liquid interfaces. The calculated interfacial free energies at coexistence per unit area for the different directions are

$$\begin{aligned}\gamma_{001} &= 0.0417\,kT_{tr}a^{-2}\\ \gamma_{011} &= 0.0464\,kT_{tr}a^{-2}\\ \gamma_{111} &= 0.0507\,kT_{tr}a^{-2}.\end{aligned} \tag{17}$$

Figure 3 shows that the critical nucleus has more surface in the [001] direction, which has the lowest interfacial free energy.

The interfacial profile for the [001] direction is different from those for the other two directions, as can be seen from figure 4. The order parameter profile has a smooth hyperbolic tangent shape in the [011] and [111] directions, but it falls sharply at the interface in the [001] direction. This is closely related to the behaviour for the (001) surface being different from that for the others, as will be discussed below. The fact that the [001] direction is different can be understood if one looks at figure 1 more closely. In the [001] direction, an atom in the top layer has its nearest neighbours in the same and the second layer, but the order parameter is not defined for the second layer which has only Cu sites. Therefore, the change of order in the top layer will have a very small effect on the order parameter for the third layer, which is the closest layer where that order parameter is defined. The composition change can propagate through the Cu layer, however. The order parameter can propagate well in the other directions because an atom in a Cu–Au layer has a nearest neighbour in the next Cu–Au layer in the [011] direction, and all layers have Cu and Au sites in the [111] direction.

3.2. Surface transitions

Before discussing nucleation at the free surface, let us look at equilibrium behaviour. As discussed in subsection 2.2, there are two additional parameters to be determined in the surface problem: the surface field $F/V^{(2)}$ and the surface enhancement $I/V^{(2)}$ (see equation (8)). The effective three-body interaction potential $V^{(3)}/V^{(2)}$ is fixed at 0.1 as before. Upon examining the phase diagram in parameter space, we chose sets of physically reasonable values for the parameters; nucleation in those model systems is discussed in the next subsection.

A phase diagram for the (001) surface in F–I parameter space is shown in figure 5. The region $0.2 < F/V^{(2)} < 0.6$ is considered because F should be positive in order to obtain Au segregation at the surface, as in experiment, and if $F/V^{(2)} > 0.6$, the third layer in the disordered state is ordered. There are three regions of different surface transition in the phase diagram. For a smaller F and I, the surface undergoes a continuous transition, but completely disorders below the bulk transition temperature (T_{bulk}). In this case, a few layers below the surface can undergo second-order transitions at different temperatures if F and I are very small. The same was seen in a cluster variation calculation [25] where $F = I = 0$ was chosen implicitly. For a larger F and I, the surface becomes more ordered and can undergo a first-order transition at T_{bulk}, and for an even larger F and I the surface does not disorder completely even above T_{bulk}, and $T_{surf} > T_{bulk}$. The transition of the (001) surface is second order at T_{bulk}, as found experimentally, only along the full line shown in figure 5. The surface Au concentration along the line at the transition temperature is shown in the inset of figure 5. The Au concentration is somewhat smaller than the experimentally determined value of $\sim$0.45 [9, 27], but it becomes higher for a larger $V^{(3)}/V^{(2)}$. The parameters fit the experiments only in a narrow range, even if one considers the experimental uncertainties.

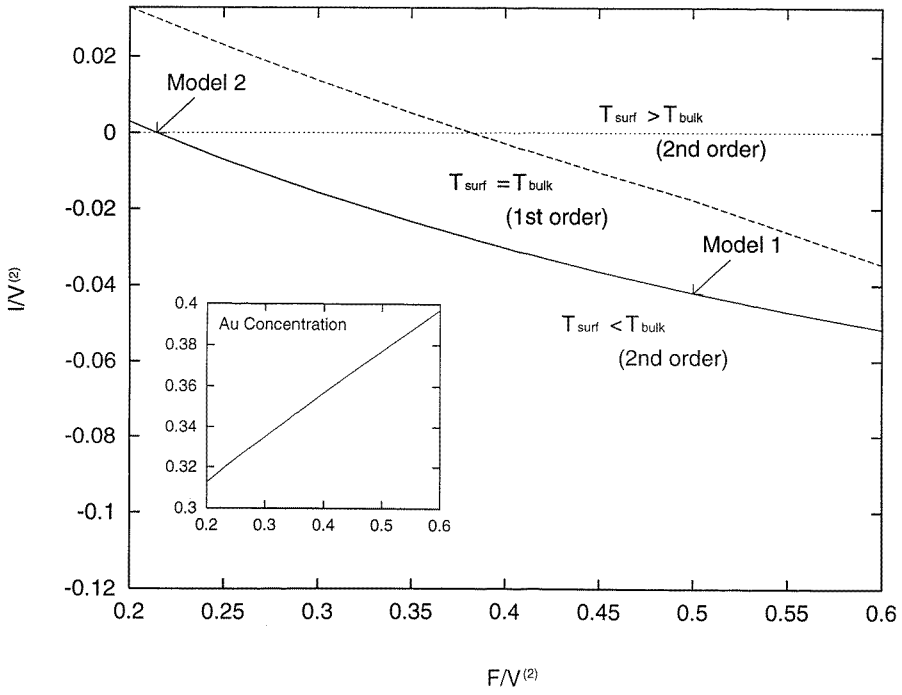

Figure 5. The phase diagram for the transition at the (001) surface. The surface transition is second order and $T_{surf} = T_{bulk}$ along the full line. The inset shows the Au concentration at the surface at T_{tr} along the full line. 'Model 1' and 'Model 2' are the sets of parameters for which nucleation calculations are performed.

A surface-induced disorder transition was not obtained for any set of parameters. Only a few subsurface layers are disordered, and the number of disordered layers does not increase even very close to the transition temperature. The order parameter profiles are shown in figure 6 for the two parameter sets ('Model 1' and 'Model 2') indicated by diamonds in figure 5:

Model 1: $F/V^{(2)} = 0.5$, $I/V^{(2)} = -0.042$; and
Model 2: $F/V^{(2)} = 0.2145$, $I/V^{(2)} = 0$.

The nucleation calculations discussed below are carried out for these two models.

The (011) and (111) surfaces undergo a surface-induced disorder transition for some choices of parameters. For example, for a (011) surface with $F/V^{(2)} = 0.1$ (for a (111) surface with $F/V^{(2)} = 0.4$), surface-induced disordering occurs if $I/V^{(2)} < -0.1$ (0.28), surface-induced ordering occurs if $I/V^{(2)} > 0.8$ (0.8), and the surface undergoes a first-order transition at T_{bulk} in between. Au segregates at these surfaces, and its fractional abundance is $\sim$0.3 for the above parameters (the experimental value is $\sim$0.35 for the (011) surface [28] and larger for the (111) surface [29]). The order parameter profiles near the transition temperature are shown in figure 7 for a parameter set that gives surface-induced disordering. It can be seen from the figure that the disordered phase at the surface grows logarithmically as T_{tr} is approached. There are experimental studies for the surface transition for these two surfaces, but they are rather confusing. In LEED experiments for the (011) surface [28], the authors conclude that the surface undergoes a first-order

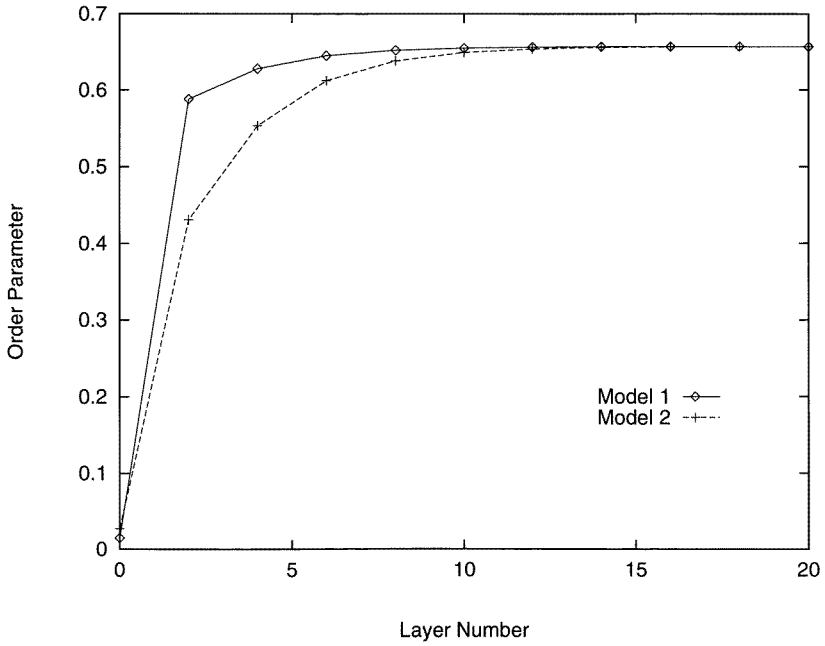

Figure 6. Order parameter profiles for model 1 and model 2 at $T = 0.9999T_{tr}$.

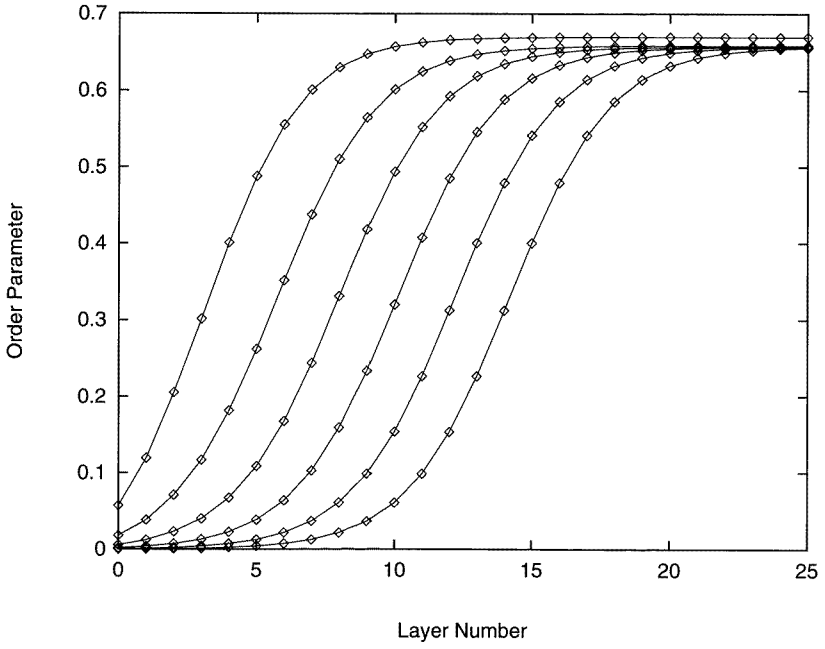

Figure 7. Order parameter profiles for a (111) surface at temperatures $(T_{tr} - T)/T_{tr} = 10^{-2}$, 10^{-3}, 10^{-4}, 10^{-5}, 10^{-6}, and 10^{-7} from the left. The parameters used are $F/V^{(2)} = 0.4$ and $I/V^{(2)} = 0$.

transition below T_{bulk} because of the presence of hysteresis and the asymmetry of the ordering and disordering rates. However, in a spin-polarized LEED study [4], a surface critical exponent for the surface-induced disorder transition was determined. The (111) surface exhibits enhanced ordering according to an x-ray study [12], but this is presumably a nonequilibrium phenomenon [10].

Why the (001) surface does not undergo a surface-induced disorder transition whereas the (011) and the (111) surfaces can in our nearest-neighbour potential model is explained at the end of the previous subsection. The (001) surface is only weakly coupled to the bulk because it does not interact with the layers beyond the next layer, which is a Cu layer. The energy of interaction between a Cu layer and a Cu–Au layer does not depend very much on whether the Cu–Au layer is more ordered or not, because a Cu layer has mostly Cu atoms in it. One might think that the (001) surface could then undergo a surface-induced disorder transition if next-nearest-neighbour interactions were included. This is true, but one cannot match the experimental results by varying the parameters. Cu segregates at the surface if a surface-induced disordering occurs and the surface ends with a Cu–Au layer [26]. One can obtain surface-induced disordering and Au segregation only when the surface is a Cu layer instead of a Cu–Au layer, contrary to experiment.

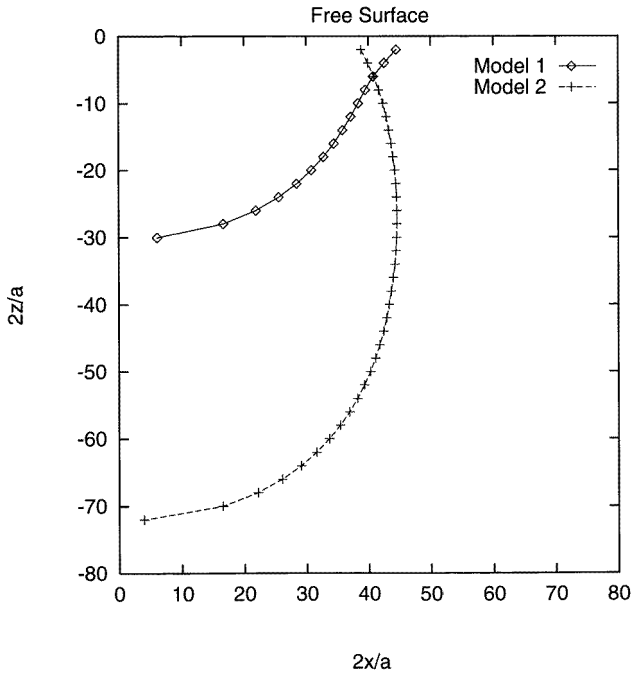

Figure 8. Sections of contours of constant order parameter cut perpendicularly to the surface and parallel to a (010) plane for critical surface nuclei at $T = 0.986T_{tr}$. The $z = 0$ plane is the free surface. The classical contact angles are 56° (model 1) and 125° (model 2).

3.3. Surface nucleation

We calculated nucleation barriers at the (001) surface for model 1 and model 2, as mentioned above. Model 1 gives sharp order parameter profiles and strong Au segregation, whereas

model 2 gives more disordered layers and weaker Au segregation, as in figures 6 and 7. The contact angles from equation (14) for ordered nuclei in the metastable disordered phase are 56° for model 1 and 125° for model 2, where γ_{001} is used for $\gamma_{\alpha\beta}$. Figure 8 shows profiles, calculated from density functional theory, for critical nuclei formed at the surface for a small undercooling, and the shape is consistent with the classical picture. The contact angles for the superheated case are 180° minus the above angles because $\cos\theta$ changes its sign in this case. It then follows that in a surface-induced disorder transition, the contact angle is 180° for ordering because $\theta = 0°$ for disordering, and surface nucleation is not favoured.

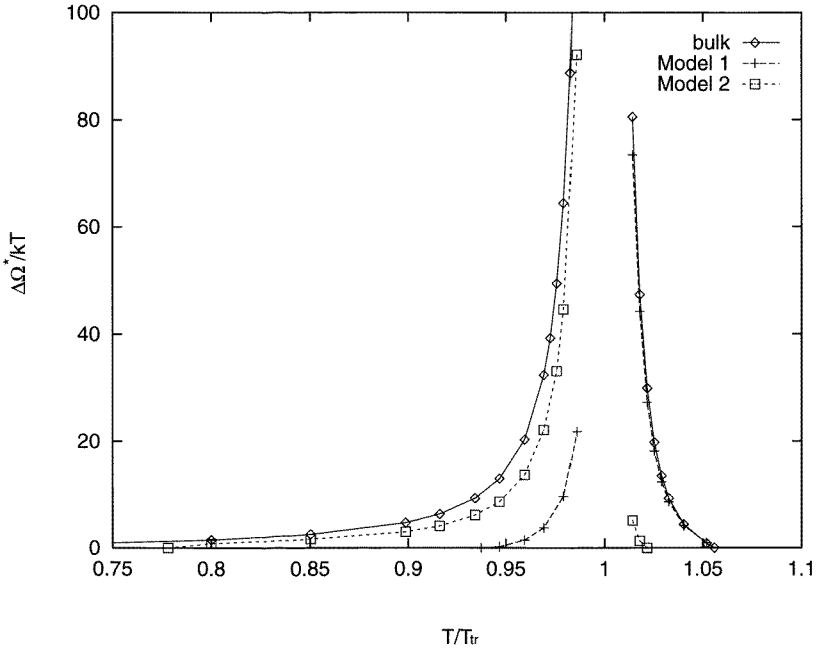

Figure 9. Nucleation barriers in bulk and at the (001) surface for two models.

It is possible for a metastable system to lose its stability from the surface at some temperature if a free surface exists. This temperature is the surface spinodal, and the surface nucleation barrier vanishes at this temperature. For the (001) surface, both model 1 and model 2 give lower and upper surface spinodals, as in figure 9. In general, the surface spinodal approaches T_{tr} as the classical contact angle becomes smaller. We obtain a lower surface spinodal even for a surface-induced disorder transition where ordering at the surface is strongly disfavoured around the transition temperature. For the (011) surface, the surface spinodal appears at $(T_{tr} - T_{sp})/T_{tr} = 0.39$ when $F/V^{(2)} = 0.1$ and $I/V^{(2)} = -0.3$, for example. The upper spinodal for a surface-induced disorder transition appears right at the transition temperature, and superheating is not possible.

We found that the nucleation barrier at the (001) surface is always smaller than that in bulk (figure 9). There is an asymmetry in the nucleation barrier for undercooling and superheating. For example, model 1 has lower barriers than model 2 when undercooled, but higher ones when superheated. Because model 2 gives more-disordered subsurface layers at equilibrium, it would be easier for a superheated sample with partially disordered layers to relax to the disordered phase. When parameters that give a surface-induced disorder

transition are used, the initial profile for an ordered nucleus is detached from the surface as one refines the guess to find a saddle point, and it is concluded that surface nucleation does not occur except near the surface spinodal. This agrees with the classical picture where the contact angle is 180°. This does not mean that the growth of the ordered phase should begin deep in the bulk. A critical nucleus can form just under the surface with the same barrier as in bulk, and the relative nucleation rate will depend on the two diffusion constants near the surface and in bulk.

The surface dynamics of Cu_3Au has been studied experimentally for all the three surfaces, although the data are limited. In helium scattering experiments for the (001) surface [5], the surface superlattice peak appeared immediately upon very shallow quenching, which implies very fast nucleation for ordering, in contrast to the slow nucleation in bulk. No hysteresis was found [2] when a sample was heated and cooled. This may occur either because both the disordering upon superheating and ordering upon undercooling are fast or because the system remains in a superheated state because the disordering is slow, and rapidly relaxes without nucleation upon cooling. These experimental results agree better with the nucleation results for model 1, which is expected to be closer to a real system than model 2 in view of the equilibrium properties. Considering the fact that the bulk nucleation rate is of the order of 1 cm^{-3} s^{-1} when the nucleation barrier $\Delta\Omega^*/kT \approx 40$, one can see from figure 9 that the surface nucleation upon undercooling is very fast even very close to T_{tr}.

Quenching experiments for the (011) surface have been done only for deep quenches where both bulk and surface nucleation are very fast [16]. The ordering rate at the surface is comparable to that in the bulk, but this cannot be explained in terms of nucleation alone because the timescale is much longer than that for nucleation. In contrast to the case for the (001) surface, hysteresis was observed [28]; surface order decreases down to zero at the bulk transition temperature when the sample is heated, but it increases very slowly upon cooling. For the (111) surface, a long incubation time was observed before the superlattice peak gained some intensity upon very shallow quenching [11]. The above results for the (011) and (111) surfaces are consistent with a surface-induced disorder transition where nucleation is very slow when a sample is undercooled.

4. Conclusions

We have studied the role of a free surface in the order–disorder transition in Cu_3Au. In the surface-induced disorder transition, the surface disorders continuously, and induces bulk disorder as temperature is increased. One might think that the surface nucleation barrier should be zero because the surface undergoes a second-order transition. However, this may not be the case because the bulk transition is first order, and there are layers below the surface that undergo first-order transitions. New-phase fluctuations at the surface may be destabilized by the unfavourable interaction with the layers below, but induce bulk transition beyond the spinodal. As discussed above, the ordering rate is determined by the bulk nucleation barrier in the surface-induced disorder transition. The nucleation barrier at the (001) surface is lower than bulk.

The (001) surface dose not induce bulk disorder within the nearest-neighbour potential model. However, Dosch and co-workers [10] measured depth-resolved order parameters down to $(T_{tr} - T)/T_{tr} \approx 10^{-3}$, and explained their results in terms of a surface-induced disorder transition. Although our results agree well with dynamics experiments for the (001) surface, there might be weak longer-range interactions responsible for the surface-induced disordering, even though the inclusion of second-nearest-neighbour interactions alone cannot

satisfy the experimental results, as discussed above. In view of the fact that the surface spinodal can exist even in the surface-induced disorder transition, surface nucleation faster than bulk nucleation for shallow quenching might be obtained for very weak long-range interactions.

Acknowledgments

This work was supported by the National Science Foundation through grant CHE 9422999 and through the Materials Research Science and Engineering Center at the University of Chicago.

References

[1] Sundaram V S, Alben R S and Robertson W D 1974 *Surf. Sci.* **46** 653
[2] McRae E G and Malic R A 1984 *Surf. Sci.* **148** 551
[3] Jamison K D, Lind D M, Dunning F B and Walters G K 1985 *Surf. Sci.* **159** L451
[4] Alvarado S F, Campagna M, Fattah A and Uelhoff W 1987 *Z. Phys.* B **66** 103
[5] King S F 1993 *PhD Thesis* The University of Chicago, IL
[6] Keating D T and Warren B E 1951 *J. Appl. Phys.* **22** 286
[7] Feder R, Mooney M and Nowick A S 1958 *Acta Metall.* **6** 266
[8] Lipowsky R and Speth W 1983 *Phys. Rev.* B **28** 3983
Lipowsky R 1984 *J. Appl. Phys.* **55** 2485
Lipowsky R 1987 *Ferroelectrics* **73** 69
[9] Buck T M, Wheatley G H and Marchut L 1983 *Phys. Rev. Lett.* **51** 43
[10] Dosch H, Mailander L, Reichert H, Peisl J and Johnson R L 1991 *Phys. Rev.* B **43** 13 172
[11] Zhu X-M, Robinson I K, Vlieg E, Zabel H, Dura J A and Flynn C P 1989 *J. Physique Coll.* **50** C7 283
[12] Zhu X-M, Feidenhans'l R, Zabel H, Als-Nielsen J, Du R, Flynn C P and Grey F 1988 *Phys. Rev.* B **37** 7157
[13] Shannon R F Jr, Nagler S E, Harkless C R and Nicklow R M 1992 *Phys. Rev.* B **46** 40
[14] Kawasaki K, Yalabik M C and Gunton J D 1978 *Phys. Rev.* A **17** 455
[15] Lai Z-W 1990 *Phys. Rev.* B **41** 9239
[16] McRae E G and Malic R A 1990 *Phys. Rev.* B **42** 1509
McRae E G and Malic R A 1990 *Phys. Rev. Lett.* **65** 737
[17] Seok C and Oxtoby D W 1997 *J. Phys.: Condens. Matter* **9** 87
[18] Nieswand M, Dieterich W and Majhofer A 1993 *Phys. Rev.* E **47** 718
Nieswand M, Majhofer A and Dieterich W 1993 *Phys. Rev.* E **48** 2521
[19] Oxtoby D W and Evans R 1988 *J. Chem. Phys.* **89** 7521
[20] Zettlemoyer A C 1969 *Nucleation* (New York: Dekker)
[21] Borg R J and Dienes G J 1992 *The Physical Chemistry of Solids* (San Diego, CA: Academic)
[22] Ludwig K F Jr, Stephenson G B, Jordan-Sweet J L, Mainville J, Yang Y S and Sutton M 1988 *Phys. Rev. Lett.* **61** 1859
[23] Chen H, Cohen J B and Ghosh R 1977 *J. Phys. Chem. Solids* **38** 855
[24] Torii K, Tamaki T and Wakabayashi N 1990 *J. Phys. Soc. Japan* **59** 3620
[25] An G and Schick M 1988 *J. Phys. A: Math. Gen.* **21** L213
[26] Kroll D M and Gompper G 1987 *Phys. Rev.* B **36** 7078
[27] Reichert H, Eng P J, Dosch H and Robinson I K 1995 *Phys. Rev. Lett.* **74** 2006
[28] McRae E G, Buck T M, Malic R A and Wallace W E 1990 *Surf. Sci.* **238** L481
[29] McDavid J M and Fain S C Jr 1975 *Surf. Sci.* **52** 161